

Article Info

Received: 25 Jun 2017 | Revised Submission: 20 Jul 2017 | Accepted: 28 Jul 2017 | Available Online: 15 Sept 2017

Numerical Prediction of Young's Modulus of MWCNTs/MnO₂ Nanocomposite

Md Zakir Hussain, Mohd Shuaib**, Urfi Khan*** and Bhaskarjyoti Pathak*****

ABSTRACT

This paper presents numerical analysis of Young's modulus of MWCNTs/MnO₂ nanocomposite. The solution method has been used to fabricate of 5, 10 and 15 wt% of MWCNTs/MnO₂ nanocomposite powder. The Young's modulus of MWCNTs/MnO₂ nanocomposites was determined using analytical models include Voigt and Reuss bounds, Hashin and Shtrikman bounds, Halpin-Tsai model, Hui-Shia model. Voigt upper bound, Halpin-Tsai and Hui-Shia models predict nearly same Young's modulus of MWCNTs/MnO₂ nanocomposite in longitudinal direction. The various models also indicate that incorporating MWCNTs in MnO₂ matrix can potentially improve mechanical properties composites significantly. Halpin and Tsai proposed the equations for discontinuous short CNTs, randomly oriented in a matrix; the effective Young's modulus of the nanocomposite also increases with wt% of MWCNTs.

Keywords: *Multi-Walled Carbon Nanotubes (MWCNTs); Manganese Di-Oxide (MnO₂); Voigt and Reuss Model; Hashin and Shtrikman Bounds; Halpin-Tsai; Hui-Shia Model etc.*

1.0 Introduction

The discovery of carbon nano-tubes by Sumio Iijima in 1991 [1], it has high aspect ratio, large surface area, low density, excellent mechanical, electrical, thermal and tribological properties have attracted researchers used as a filler material nano-composite material. Composite materials with at least one of their constituent being less than 100 nm are commonly known as nano-composites. The experimental based research can ideally be used to determine the elastic properties of nano-composites, with the help of advanced fabrication process and testing equipment. Computational approach can play a vital role in the development of CNT based nano-composites and requires proper selection of mathematical models for the materials under investigation.

Manganese dioxide is used because of its low cost, eco friendly [2] and its electronic structure can exhibit metallic, semiconductor, or insulator behaviour. Most of the literature related to electrical properties of CNT/MnO₂ nano-composite, continuous

study of the mechanical properties of the nano composite could lead to useful multifunctional materials with simultaneous mechanical and electrochemical properties. So in near future manganese dioxide can be widely use as an engineering material. Hurang Hu et al. presented a critical review of recent experimental work, theory of micro nano-mechanics, and numerical analysis on mechanical properties of nano-composites material [3]. Amir Mostafa et al. [4] fabricated thermoplastic polyolefin elastomeric nano composites and investigated the effect of different pin geometries on clay dispersion. They applied three micromechanical models Halpin-Tsai, inverse rule of mixture and linear rule of mixture to investigate the Young's modulus of nano composites. They found that there was a significant difference between the Young's modulus obtained from these models and that obtained from experimental value. Hong Gun Kim et al. derived a closed form solution of the shear lag theory and predicted elastic modulus of short fiber reinforced discontinuous composite materials [5] and derive an analytical model for the stress transfer in

*Corresponding Author: Department of Mechanical Engineering, Jamia Millia Islamia, New Delhi, India
(E-mail: mechazakirhussain@gmail.com)

**Department of Mechanical Engineering, DTU, New Delhi, India

***Department of Mechanical Engineering, IGDTUW, New Delhi, India

****Department of Mechanical Engineering, Goalpara Polytechnic, Assam India

acomposite. The predictions of the theoretical model to predict the composite Young's modulus are fairly consistent with the experimental result of SiC-Al metal matrix composite. In this study, a numerical prediction of Young's modulus of MWCNTs/ MnO₂ nanocomposites is done.

2.0 Mathematical Modelling

2.1 Mathematical modelling of nanocomposites

Many models can be applied to describe the effect of carbon nanotubes on composite materials. Common models are Voigt and Reuss bounds, Hashin and Shtrikman bounds, Halpin-Tsai model, Hui-Shia models.

2.2 Numerical analysis of young's modulus of MWCNTs/ MnO₂ nano composite

2.2.1 Voigt upper bound and Reuss lower bound

Voigt assumed that the reinforcement material and matrix are subjected to equal uniform strain in the fiber direction and predicted Young's modulus in the fiber direction called rule of mixture upper bound Equation and also known as the parallel coupling formula as shown (1) [7]

$$E_L = \phi_{MWCNTs} \times E_{MWCNTs} + (1-\phi) \times E_{MnO_2} \quad (1)$$

Where E is the Young's modulus and ϕ is the volume fraction of reinforcement material

Reuss applied the same uniform stress in the transverse direction, and predicted the modulus in the transverse direction called inverse rule of mixtures, also known as series coupling formula as shown (2) [8]:

$$E_T = \frac{1}{\left(\frac{\phi_{MWCNT}}{E_{MWCNT}} + \frac{\phi_{MnO_2}}{E_{MnO_2}}\right)} \quad (2)$$

2.2.2 Hashin and shtrikman upper and lower bounds

Hashin and Shtrikman [9] assumed that the material is macroscopically isotropy and homogeneous, and predicted the elastic constant of the composite are as given below

The upper bound Bulk modulus as shown (3)

$$k_{upper} = k_f + (1-\phi) \frac{1}{\left[\frac{1}{k_m - k_f} + \frac{3\phi}{3k_f + 4G_f}\right]} \quad (3)$$

The lower bound bulk modulus as shown (4)

$$k_{lower} = k_m + \phi \frac{1}{\left[\frac{1}{k_f - k_m} + \frac{3(1-\phi)}{3k_m + 4G_m}\right]} \quad (4)$$

The upper bound shear modulus as shown (5)

$$G_{upper} = G_f + (1-\phi) \frac{1}{\left[\frac{1}{G_m - G_f} + \frac{6\phi(k_f + 2G_f)}{5G_f(3k_f + 4G_f)}\right]} \quad (5)$$

The lower bound shear modulus as shown (6)

$$G_{lower} = G_m + \phi \times \frac{1}{\left[\frac{1}{G_f - G_m} + \frac{6(1-\phi)(k_m + 2G_m)}{5G_m(3k_m + 4G_m)}\right]} \quad (6)$$

The lower bound Young's modulus as shown (7)

$$E_{lower} = \frac{9K_{lower}G_{lower}}{3K_{lower} + G_{lower}} \quad (7)$$

The upper bound Young's modulus as shown (8)

$$E_{upper} = \frac{9K_{upper}G_{upper}}{3K_{upper} + G_{upper}} \quad (8)$$

2.2.3 Halpin-tsai model

Halpin and Tsai [10, 11] developed the equations for aligned fiber-reinforced composite materials and predicted the elastic modulus based Hermans and Hill equation [10].

According to Halpin-Tsai model, the longitudinal and transverse modulus is shown by (9) and (10):

$$E_L = \frac{1 + 2\left(\frac{l}{d}\right)\phi\eta_L}{1 - \phi\eta_L} E_m \quad (9)$$

$$E_T = \frac{1 + 2\phi\eta_T}{1 - \phi\eta_T} E_m \quad (10)$$

Where

$$\eta_L = \frac{E_f - E_m}{E_f + 2\left(\frac{l}{d}\right)E_m}, \quad \eta_T = \frac{E_f - E_m}{E_f + 2E_m}$$

When the reinforcing materials are discontinuous short CNTs, randomly oriented in a matrix, Halpin and Tsai proposed the equations to estimate the effective Young's modulus as [12]

$$E_{em} = \frac{3}{8} E_L + \frac{5}{8} E_T$$

2.2.4 Hui-shia model

Hui and Shia and Shia et al. [13] derived formulas for predicting the overall modulus of composites with aligned reinforcements with fiber and flake like reinforcements. They found that the theoretical predictions agreed with experimental results. The Hui-Shia model presents the Young's modulus as shown by equation (11) and (12)

$$E_L = E_m \left[\frac{1-\phi}{1-\frac{\phi}{\xi}} \right] \quad (11)$$

$$E_T = E_m \left[\frac{1}{1 - \frac{\phi}{4} \left(\frac{1}{\xi} + \frac{3}{\xi + \lambda} \right)} \right] \quad (12)$$

Where

$$\xi = \varphi + \frac{E_m}{E_f + E_m} + 3(1 - \varphi) \left[\frac{(1-g)\alpha^2 - \frac{g}{2}}{\alpha^2 - 1} \right]$$

$$\Lambda = (1 - \varphi) \left[\frac{3(\alpha^2 + 0.25)g - 2\alpha^2}{\alpha^2 - 1} \right]$$

$$g = \frac{\alpha}{(\alpha^2 - 1)^{3/2}} \left[\alpha \sqrt{\alpha^2 - 1} - \cosh^{-1} \alpha \right]$$

3.0 Materials and Synthesis of Nano-Composite

3.1 Materials

The reinforcing material used was Multiwall Carbon nanotubes and KMnO₄ used as oxidising agent.

3.2 Synthesis of 10 wt% MWCNTs/ MnO₂ nanocomposite

The solution method [15, 16] has been applied to fabricate MWCNTs/MnO₂ nanocomposite powder. In shortly the process is described as--

In a beaker, 0.2 gram multi wall nano-tube immersed in 2M boiling H₂SO₄ (aq) solution. After 3 hours of dispersion, 4 gram KMnO₄ was added at 85°C.

The solution color changed from purple to brown and precipitates was obtained.

The obtained black yield was washed with de-ionized water and then dried at 65°C in a laboratory oven for 4 hours. The obtained black yield was 2.03 g.

Similar, the experiments were carried out for 5 wt% and 15 wt% MWCNTs/MnO₂ nanocomposites powder.

The yield obtained were 1.96gm, 2.03 gm and 2.14 gm for 5 wt%, 10 wt% and 15 wt% of MWCNTs/ MnO₂ nanocomposites powder respectively as shown in figure 1.

4.0 Chemical Characterization

The chemical structure of the nano-composite was investigated using Mini Flex, with Cu-K α radiation. The XRD pattern of the MWCNTs is as shown in figure 2. Diffraction peaks at 26.550 can be indexed as (002) plane and it is also reflections of graphite [15, 16, and 17].

The other diffraction peaks can be indexed to the tetragonal α -MnO₂, group: I4/m (87 as shown in fig:3.

It is confirmed that the MWCNTs/MnO₂ nano-composite is formed and MnO₂ as a single crystal structure called α -MnO₂ [14, 15].

Fig 1: Yield of Different wt% MWCNTs/MnO₂ Nano-Composite Powder.



Fig 2: XRD Pattern of MWCNTs

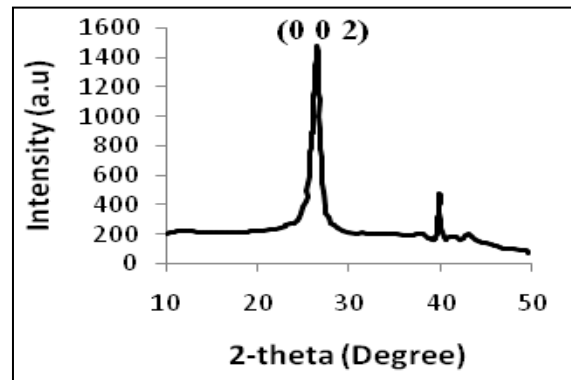
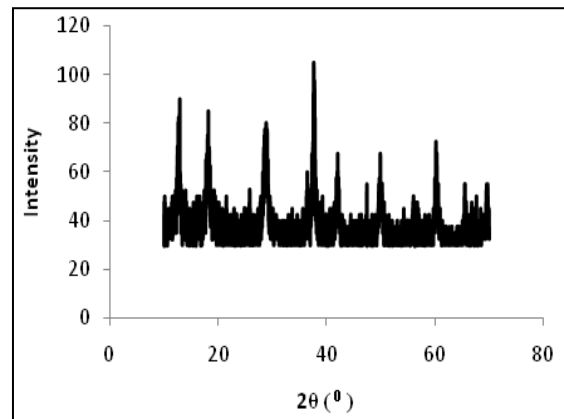


Fig 3: XRD Pattern of 10 wt% MWCNTs/MnO₂



5.0 Result and Discussion

5.1 Elastic constants of MWCNTs and MnO₂

Table 1 and Table 2 shows the physical and mechanical properties of MWCNTs and MnO₂

Table 1: Properties of MWCNTs Synthesized by CVD

Parameter	Properties
Density g/cm ³	1.33-1.4[15,17,18]
Young's modulus TPa	0.45[15,17]
Poisson's ratio	0.14

Table 2: Properties of MnO₂

Parameter	MnO ₂ [19]
Density(ρ _m) [g/cm ³]	4.55
Poisson's ratio(μ _m)	0.28
Bulk Modulus, K [GPa]	34.4

5.1.1 Theoretical elastic constants of MWCNTS

Consider the MWCNTs are isotropic.

The Shear modulus of MWCNTs is shown (13)

$$E=2G(1+\mu) \tag{13}$$

$$G \cong 197\text{GPa}$$

Bulk modulus of MWCNTs is shown (14)

$$E=3K(1-2\mu) \tag{14}$$

$$K \cong 208.33\text{GPa}$$

5.1.2 Theoretical elastic constants of MnO₂

Young's modulus of matrix material MnO₂ is given by (E_m)=3K_m(1-2μ_m)=45.40 GPa

Young's modulus of matrix material (E_m)=2G_m(1+μ_m)

$$\text{Shear modulus } (G_m) \cong 17.73 \text{ GPa}$$

5.2 Numerical determination of young's modulus of MWCNTs/ MnO₂ nano composite

5.2.1 Numerical model of 5% MWCNTs/MnO₂ nano composite

5.2.1.1 Volume fraction of MWCNTs

The yield 5 wt% MWCNTs/MnO₂ nano composite was obtained 1.96g by using solution method.

$$\text{Volume of MWCNTS } (V_f) = \frac{m_f}{\rho_f} = \frac{0.1}{1.34} = 0.07462$$

$$\text{Vol. of MnO}_2 (V_m) = \frac{m_m}{\rho_m} = \frac{1.86}{4.55} = 0.4087$$

$$\text{Volume fraction of MWCNTS } (\varphi) = \frac{V_f}{V_m + V_f} = \frac{0.07462}{0.07462 + 0.4087} = 0.15388$$

5.2.1.2 Young's Modulus of 5% wt MWCNTs/MnO₂ nanocomposite

5.2.1.2.1 Voigt upper bound and Reuss lower bound model

Longitudinal Young's modulus of 5 wt% MWCNTs/MnO₂ nanocomposite

$$E_{LC} = \varphi E_{MWCNTS} + (1-\varphi) E_{MnO2} = 107.65\text{GPa}$$

Transverse Young's modulus of 5 wt% MWCNTs/MnO₂ nano-composite

$$E_{TC} = \frac{1}{\left(\frac{\varphi}{E_{MWCNT}} + \frac{1-\varphi}{E_{MnO2}}\right)} = 52.70 \text{ GPa}$$

5.2.1.2.2 Hashin and Shtrikman upper and lower bounds

$$k_{upper} = k_f + (1 - \varphi)k_m = 208.33 + (1 - 0.15439) \frac{1}{\frac{1}{34.4 - 208.33} + \frac{3 \times 0.15439}{3 \times 208.33 + 4 \times 197.36}} = 52.36 \text{ GPa}$$

$$k_{lower} = k_m + \varphi \frac{1}{\left[\frac{1}{k_f - k_m} + \frac{3(1-\varphi)}{3k_m + 4G_m}\right]} = 34.4 + 0.15439 \frac{1}{\frac{1}{208.33 - 34.4} + \frac{3(1-0.15439)}{3 \times 34.4 + 4 \times 17.33}} = 42.0 \text{ GPa}$$

$$G_{upper} = G_f + (1 - \varphi) \frac{1}{\left[\frac{1}{G_m - G_f} + \frac{6\varphi(k_f + 2G_f)}{5G_f(3k_f + 4G_f)}\right]}$$

$$= 197.36 + (1 - 0.15439) \frac{1}{\left[\frac{1}{17.73 - 197.36} + \frac{6 \times 0.15439(208.33 + 2 \times 197.36)}{5 \times 197.36(3 \times 208.33 + 4 \times 197.36)}\right]} = 33.696 \text{ GP}$$

$$G_{lower} = G_m + \varphi \times \frac{1}{\left[\frac{1}{G_f - G_m} + \frac{6(1 - \varphi)(K_m + 2G_m)}{5G_m(3k_m + 4G_m)}\right]} G_{lower} = 17.73 + 0.15439$$

$$\times \frac{1}{\left[\frac{1}{197.36 - 17.73} + \frac{6(1 - 0.15439)(34.4 + 2 \times 17.73)}{5 \times 17.73(3 \times 34.4 + 4 \times 17.73)}\right]} = 83.23 \text{ GPa}$$

$$E_{\text{lower}} = \frac{9K_{\text{lower}}G_{\text{lower}}}{3K_{\text{lower}} + G_{\text{lower}}}$$

$$E_{\text{lower}} = \frac{9 \times 42 \times 23.14}{3 \times 42 + 23.14} = 58.64 \text{ GPa}$$

$$E_{\text{upper}} = \frac{9K_{\text{upper}}G_{\text{upper}}}{3K_{\text{upper}} + G_{\text{upper}}} = 83.23 \text{ GPa}$$

5.2.1.2.3 Halpin-tsai model

$$\eta_L = \frac{E_f - E_m}{E_f + 2\left(\frac{l}{d}\right)E_m} \eta_L$$

$$= \frac{0.45 \times 10^3 - 45.40}{.45 \times 10^3 + 2 \times 1000 \times 45.40}$$

$$= 4.4339 \times 10^{-3}$$

$$\eta_T = \frac{E_f - E_m}{E_f + 2E_m} \eta_T = \frac{0.45 \times 10^3 - 45.40}{0.45 \times 10^3 + 2 \times 45.40} = 0.74815$$

$$E_L = \frac{1 + 2\left(\frac{l}{d}\right)\eta_L}{1 - \eta_L} E_m =$$

$$\frac{1 + 2 \times 1000 \times 0.15439 \times 4.4339 \times 10^{-3}}{1 - 0.15439 \times 4.4339 \times 10^{-3}} = 107.62 \text{ GPa}$$

$$E_T = \frac{1 + 2\eta_T}{1 - \eta_T} E_m = \frac{1 + 2 \times 0.15439 \times 0.74815}{1 - 0.15439 \times 0.74815} \times 45.40$$

$$= 63.186 \text{ GPa}$$

When the reinforcing materials are discontinuous short CNTs, randomly oriented in a matrix, Halpin and Tsai proposed the equations for discontinuous short CNTs, randomly oriented in a matrix to estimate the effective Young's modulus

$$E_m = \frac{3}{8} E_L + \frac{5}{8} E_T = \frac{3}{8} \times 107.62 + \frac{5}{8} \times 63.186 = 79.848 \text{ GPa}$$

5.2.1.2.4 Hui-Shia model

$$\xi = \phi + \frac{E_m}{E_f + E_m} + 3(1 - \phi) \left[\frac{(1-g)\alpha^2 - \frac{g}{2}}{\alpha^2 - 1} \right]$$

$$\xi = 0.15439 + \frac{45.40}{450 + 45.40} +$$

$$3(1 - 0.15439) \left[\frac{(1 - 0.9999)1000^2 - \frac{0.9999}{2}}{1000^2 - 1} \right] = 0.26684$$

$$\Lambda = (1 - \phi) \left[\frac{3(\alpha^2 + 0.25)g - 2\alpha^2}{\alpha^2 - 1} \right] = (1 -$$

$$0.15439) \left[\frac{3(1000^2 + 0.25)0.9999 - 2 \times 1000^2}{1000^2 - 1} \right] = 0.84535$$

$$g = \frac{\alpha}{(\alpha^2 - 1)^{3/2}} [\alpha \sqrt{\alpha^2 - 1} -$$

$$\cosh^{-1} \alpha] = \frac{1000}{(1000^2 - 1)^{3/2}} [1000 \sqrt{1000^2 - 1} -$$

$$\cosh^{-1} 1000] = 0.9999$$

$$E_L = E_m \left[\frac{1}{1 - \frac{\phi}{\xi}} \right] = 45.40 \left[\frac{1}{1 - \frac{0.15439}{0.26684}} \right] = 107.73 \text{ GPa}$$

$$E_T = E_m \left[\frac{1}{1 - \frac{\phi}{\frac{1}{4}\xi + \xi + \Lambda}} \right] =$$

$$45.40 \left[\frac{1}{1 - \frac{0.15439}{4 \left(\frac{1}{0.26684} + \frac{3}{0.26684 + 0.84535} \right)}} \right] = 60.44 \text{ GPa}$$

Similarly, the theoretical Young's modulus of 10 and 15 wt% were calculated. Table:3 shows the

theoretical Young's modulus of MWCNTs/MnO₂ nanocomposites calculated using different models.

Table 3: Theoretical Young's Modulus of MWCNTs/ MnO₂ Nano-Composites

Model	5wt% MWCNTs/MnO ₂ nanocomposite	10 wt% MWCNTs/MnO ₂ nanocomposite	15 wt% MWCNTs/MnO ₂ nanocomposite
Voigt upper bound and Reuss lower bound model	EL=107.65GPa	EL=154.88GPa	EL= 189.55GPa
	ET=52.70 GPa	ET=59.99 GPa	ET=66.79 GPa
Hashin and Shtrikman upper and lower bounds	E _{lower} =58.64GPa	E _{lower} =71.63GPa	E _{lower} =83.03
	E _{upper} =83.23 GPa	E _{upper} =115.27 GPa	E _{upper} =141.35
Halpin-Tsai model	E _L =107.47	E _L =154.158	E _L =189.144
	E _T =63.186GPa	E _T =79.97GPa	E _T =94.90
Halpin-Tsai model (discount. randomly oriented fiber)	E _m =79.848 GPa	E _m =107.92	E _m =130.241
Hui-Shia model	E _L =107.73	E _L =154.69	E _L =189.32
	E _T =60.44	E _T =75.469	E _T =79.699

Fig 4: Variation of Longitudinal Young's Modulus with wt% of MWCNTS

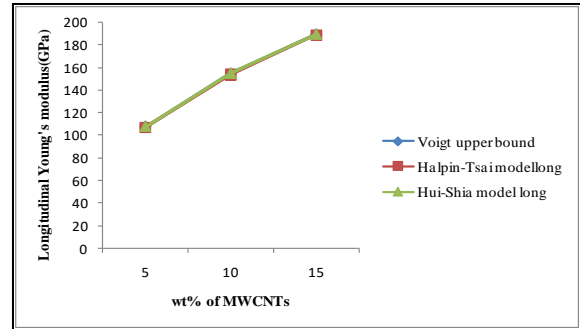
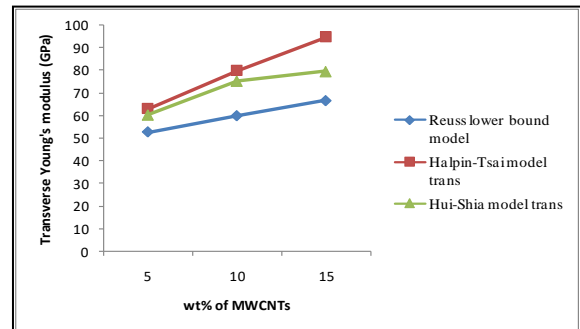


Fig 5: Variation of Transverse Young's Modulus with wt% of MWCNTS



5.3 Variation of young's modulus with wt% of MWCNTs

The Young's modulus in longitudinal direction is nearly same for the models Voigt upper bound Halpin-Tsai and Hui-Shia. But it is slightly different in transverse direction. The variation of Young's modulus in longitudinal and transverse direction is shown in figure 4 and figure 5 respectively. These three models may be conveniently used to determine Young's modulus of MWCNTs/MnO₂ nanocomposite in longitudinal direction.

6.0 Conclusions

In the present work, numerical analysis of Young's modulus of MWCNTs/MnO₂ nanocomposite at different weight fraction of MWCNTs varying from 5 to 15% is investigated. It is observed that Voigt upper bound, Halpin-Tsai model and Hui-Shia models gives similar results of Young's modulus in longitudinal direction at different wt% of MWCNTs. This also shows that Voigt upper bound, Halpin-Tsai model or Hui-Shia models can only used to predict theoretical Young's modulus of MWCNTs/MnO₂ nano composite in longitudinal direction and there is a significant difference in transverse direction. The various models also indicate that incorporating MWCNTs in MnO₂ matrix can potentially improve mechanical properties composites significantly.

Acknowledgement

The authors are grateful for the discussions and comments by Mr. Swadesh Kumar Gupta, Assistant Professor, Department of Mechanical Engineering, Hi-Tech Institute of Engineering Technology, Ghaziabad, India.

References

- [1] S Iijima. Helical microtubules of graphitic carbon. *Nature*, 354, 1991, 56-58
- [2] H Xia, Y Wang, J Lin, L Lu. Hydrothermal synthesis of MnO₂/CNT nanocomposite with a CNT core/porous MnO₂ sheath hierarchy architecture for super capacitors, *Nano scale research letters*, 7(1), 2012, 33-42
- [3] H Hu, L Onyebueke, A Abatan. Characterizing and modelling mechanical properties of nano-composites-review and evaluation. *Journal of minerals and materials characterization and engineering*, 9(4), 2010, 275-319
- [4] A Mostafapour, G Naderi. Theoretical models for prediction of mechanical behaviour of the PP/EPDM nanocomposites fabricated by friction stir process. *Polyolefins Journal*, 4(1), 2016, 99-109.
- [5] HG Kim, LK Kwac. Evaluation of elastic modulus for unidirectionally aligned short fiber composites. *Journal of Mechanical Science and Technology*, 23(1), 2009, 54-63.
- [6] MA Ghafaar, AA Mazen, NA El-Mahallawy, Application of the rule of mixtures and Halpin-Tsai equations to woven fabric reinforced epoxy composites. *Journal of Engineering Sciences, Assiut University*, 34, 2006, 227-236.
- [7] W Voigt. Ueber die Beziehung zwischen den beiden Elasticitäts constanten isotroper Körper. *Annalen der Physik*, 274(12), 1989, 573-587.
- [8] A Reuss. Berechnung der Fließgrenze von Mischkristallen auf Grund der Plastizitätsbedingung für Einkristalle. *Zeitschrift für Angewandte Mathematik und Mechanik*, 9(1), 1929, 49-58
- [9] Z Hashin, S Shtrikman. A variational approach to the theory of the elastic behaviour of multiphase materials. *Journal of the Mechanics and Physics of Solids*, 11(2), 1963, 127-140.
- [10] JC Affdl, JL Kardos. The Halpin-Tsai equations: a review. *Polymer Engineering & Science*, 16(5), 1976, 344-352.

- [11] JE Halpin. Revised Primer on Composite Materials: Analysis. Technomic Publishing Company, 1984
- [12] BR Reddy, K Ramji. Modeling and Simulation of Nano and Multiscale Composites. International Journal of Hybrid Information Technology, 9(3), 2016, 133-144.
- [13] D Shia, CY Hui, SD Burnside, EP Giannelis. An interface model for the prediction of Young's modulus of layered silicate-elastomer nano-composites, Polymer Composites, 19(5), 1998, 608-617
- [14] Y Chen, CG Liu, C Liu, GQ Lu, HM Cheng. Growth of single-crystal α -MnO₂ nano rods on multi-walled carbon nano tubes, Materials Research Bulletin, 42(11), 2007, 1935-1941
- [15] MZ Hussain, S Khan, R Nagarajan, U Khan, V Vats. Fabrication and Microhardness Analysis of MWCNT/MnO₂ Nanocomposite, Journal of Materials, 2016
- [16] MZ Hussain, U Khan, AK Chanda, R Jangid. Fabrication and Hardness Analysis of F-MWCNTs Reinforced Aluminium Nanocomposite. Procedia Engineering, 173, 2017, 1611–1618
- [17] SC Tjong. Carbon nanotube reinforced composites: metal and ceramic matrices. John Wiley & Sons 2009
- [18] JM Wernik, SA Meguid. Recent developments in multifunctional nano composites using carbon nanotubes. Applied Mechanics Reviews, 63(5),2010, 050801
- [19] Fraser, A., Borg, J. P., Jordan, J. L., & Sutherland, G. (2009). Exploring the micro-mechanical behavior of Al-MnO₂-epoxy under shock loading while incorporating the epoxy phase transition. In Proceedings of the SEM Annual Conference, Albuquerque New Mexico USA 2009